

Performance improvement of a novel zero cross-correlation code using Pascal's triangle matrix for SAC-OCDMA systems

Samia Driz*, Benattou Fassi, Chahinaz Kandouci, Fodil Ghali

Telecommunications and Digital Signal Processing Laboratory, Djillali Liabes University, Sidi Bel Abbas, 22000 Algeria

Article info

Article history:

Received 8 Oct. 2021

Received in revised form 11 Dec. 2021

Accepted 20 Dec. 2021

Available on-line 18 Feb. 2022

Keywords:

Multiple access interference; Pascal's triangle matrix; quality of service; spectral amplitude coding-optical code division multiple access; zero cross-correlation.

Abstract

In order to minimize the receiver complexity and improve the performance of the spectral amplitude coding - optical code division multiple access system, a novel one-dimensional zero cross-correlation code using Pascal's triangle matrix has been suggested. This research article shows that the position of chip "1" in the code sequences is one of the important factors affecting system performance. In fact, mathematical results show that, for the all-wavelength direct detection, it is possible to reduce the number of filters without sacrificing system performance. In addition, compared to one-wavelength direct detection, the signal-to-noise ratio value is increased with an increasing weight by using wide-bandwidth filters as decoders. Performance of the proposed system in terms of the minimum bit error rate is validated using the OptiSystem software. Compared with the previous systems at 622 Mbps, the suggested system gave the best values of bit error rate of around 10^{-43} , 10^{-35} , and 10^{-26} for higher, medium, and lower service demand, respectively.

1. Introduction

Nowadays, one of the most attractive multiple access techniques deployed in the world of communications is an optical code division multiple access (OCDMA). It offers a flexible sharing of a common optical spectrum between several users, simultaneous and asynchronous access, high-speed connectivity, network control and management, service differentiation, and increased security [1–3].

The OCDMA system performance depends to a large extent on several parameters such as transmission data rate, transmitter power, simultaneous number of users, and the chosen code. The capacity of OCDMA systems in terms of number of active users can be increased by using codes with large cardinality [4, 5]. On the other hand, to enhance channel data rate and increase the number of users, combining of spectral amplitude coding OCDMA (SAC-OCDMA) system with other techniques such as subcarrier multiplexing (SCM) [6] and orthogonal frequency-division multiplexing (OFDM) [7] is required. Also, in the last few years, studies have shown that OCDMA network

infrastructure is vulnerable towards several types of security attacks, such as eavesdropping where the safety component needs further safety requirements in the face of dramatic increases in network capacity [8, 9].

Nonetheless, OCDMA system performance is limited by a multiple access interference (MAI) impact. Numerous one- (1D) [10–14], two- (2D) [15–17], and three- (3D) [18] dimensional code schemes have been proposed in the literature review to eliminate the MAI where it is necessary to choose a good family of optical codes admitting a large number of users with a high weight and good auto and cross-correlation properties [less periodic cross-correlation function (PCCF) and periodic auto correlation function (PACF)].

Zero cross-correlation (ZCC) code has received great attention due to its ability to resolve the problem of spectrum overlapping and, consequently, MAI suppression [19–21]. Different construction techniques of ZCC codes are reported in the literature. Recently, Nisar [22] constructed the ZCC code using the Pascal's triangle pattern called Pascal's triangle matrix (PTM) which allows simplicity of construction, more users, and better code length than the existing codes.

*Corresponding author at: samia7922@yahoo.fr

In this research article, we propose a novel one-dimensional ZCC code using Pascal's triangle rule (ZCC-PTM). The SAC-OCDMA system performance is enhanced by using the newly constructed ZCC-PTM code instead of the existing codes with cost effectiveness. In fact, the proposed ZCC-PTM code offers several advantages such as simple construction with flexibility in choosing weight and users, low complexity receivers, and quality of service (QoS) differentiation.

The rest of this paper is organized as follows: section 2 explains the Pascal's triangle rule and describes the construction of the proposed ZCC-PTM code; section 3 presents the most salient features of the proposed code; section 4 covers performance analysis, comparison with reported codes, and discussions; section 5 presents the conclusions.

2. ZCC-PTM code construction

The PTM is defined using binary numbers ("0" and "1") and it starts from the second row where all numbers other than "1", are replaced by "0" and the outer branches of the matrix are filled with zeros [22–24]. The Pascal's type triangle matrix follows the general form defined as:

$$PTM_{m,n} = \left[\begin{array}{cccccccc} & & & \text{n-times} & & & & \\ & & & \updownarrow & & & & \\ 00 & \dots & 1 & \dots & \dots & 1 & \dots & 00 \\ \vdots & 010 & \dots & \dots & \dots & 010 & \dots & \vdots \\ \vdots & 010 & \dots & \dots & \dots & 010 & \dots & \vdots \\ 010 & \dots & \dots & \dots & \dots & 010 & \dots & \\ 10 & \dots & \dots & \dots & \dots & 01 & \dots & \end{array} \right] \text{ m-rows. } \quad (1)$$

For $m = 4$ and $n = 2$, the 4×8 PTM matrix can be written as follows:

$$PTM_{4,2} = \begin{bmatrix} 00011000 \\ 00100100 \\ 01000010 \\ 10000001 \end{bmatrix}. \quad (2)$$

Similarly, for $m = 4$ and $n = 3$, the 4×9 PTM matrix can be written as follows:

$$PTM_{4,3} = \begin{bmatrix} 000111000 \\ 001000100 \\ 010000010 \\ 100000001 \end{bmatrix}. \quad (3)$$

On the other hand, PTM has been successfully exploited for the construction of ZCC codes since there is no overlapping occurrence of chips "1" in the matrix, thus, zero cross-correlation. This means that all constructions of ZCC codes based on the PTM matrix keep the zero cross-correlation property since both matrices have the same ZCC property.

Construction steps of the proposed one-dimensional ZCC-PTM code are as follows. The proposed code is characterized by different parameters (K , w , L , and λ_c) where " K " denotes the number of users, " w " is the code weight, " L " represents the code length given as $L = K \times w$ and " λ_c " is the cross correlation of the code.

Step 1: Let us construct a 4×4 identity matrix as:

$$I_1 = \begin{bmatrix} 1000 \\ 0100 \\ 0010 \\ 0001 \end{bmatrix}_{4 \times 4}. \quad (4)$$

Step 2: The basic 4×8 ZCC-PTM ($K = 4$, $w = 2$, $L = 8$, $\lambda_c = 0$) code matrix is given by the matrix $PTM_{4,2}$ described in (2). Except for $w = 3$, the ZCC-PTM code matrix is given by:

$$ZCC - PTM_{K=4;w=3} = [I_1, PTM_{4,2}], \quad (5)$$

where $[.,.]$ means the concatenation of the two elements. Thus, $ZCC - PTM_{4,3}$ matrix can be written as follows:

$$ZCC - PTM_{4,3} = \begin{bmatrix} 1000 & 00011000 \\ 0100 & 00100100 \\ 0010 & 01000010 \\ 0001 & 10000001 \end{bmatrix}. \quad (6)$$

As presented in (7), the first column of the code matrix [see (6)] is shifted to the middle of the $PTM_{4,2}$ matrix as:

$$ZCC - PTM_{4,3} = \begin{bmatrix} 1000 & 00011000 \\ 0100 & 00100100 \\ 0010 & 01000010 \\ 0001 & 10000001 \end{bmatrix} = \begin{bmatrix} 000 & 000111000 \\ 100 & 001000100 \\ 010 & 010000010 \\ 001 & 100000001 \end{bmatrix}. \quad (7)$$

Therefore, the final form of the $ZCC - PTM_{4,3}$ code matrix is given by:

$$ZCC - PTM_{4,3} = [I_2, PTM_{4,3}]. \quad (8)$$

where $[I_2]$ consists of 4×3 matrix as following:

$$I_2 = \begin{bmatrix} 000 \\ 100 \\ 010 \\ 001 \end{bmatrix}_{4 \times 3}. \quad (9)$$

Step 3: In order to increase the weight w , a simple operation is required as shown below:

$$ZCC - PTM_{K,w} = [\text{repeat}(I_2, w - 2), PTM_{K,w}], \quad (10)$$

where $\text{repeat}(I_2, w - 2)$ denotes the replica of each element of I_2 matrix ($w - 2$) times.

Example 1

According to Step 3 [see (10)], for $K = 4$ and $w = 4$, $K \times (K * w)$ ZCC-PTM matrix is obtained where, first, each element of the I_2 matrix, given by (9), was repeated twice. Then, the resulting matrix was concatenated with the basic $PTM_{4,4}$ matrix as follows:

$$ZCC - PTM_{4;4} = \left[\text{repeat}(I_2, 2), PTM_{4;4} \right]$$

$$= \begin{bmatrix} 000000 & 0001111000 \\ 110000 & 0010000100 \\ 001100 & 0100000010 \\ 000011 & 1000000001 \end{bmatrix}_{4 \times 16}$$

To increase the number of users (codes), the size of the basic matrix (I_2 and $PTM_{K;w}$) is increased and step 3 is repeated as shown in Example 2.

Example 2

- For $K = 5$ and $w = 3$, 5×15 ZCC-PTM matrix is obtained as:

$$ZCC - PTM_{5;3} = \begin{bmatrix} 0000 & 00001110000 \\ 1000 & 00010001000 \\ 0100 & 00100000100 \\ 0010 & 01000000010 \\ 0001 & 10000000001 \end{bmatrix}_{5 \times 15}$$

- For $K = 4$ and $w = 5$, 4×20 ZCC-PTM matrix is obtained as:

$$ZCC - PTM_{4;5} = \begin{bmatrix} 000000000 & 00011111000 \\ 111000000 & 00100000100 \\ 000111000 & 01000000010 \\ 000000111 & 10000000001 \end{bmatrix}_{4 \times 20}$$

$$= \begin{bmatrix} C1 \\ C2 \\ C3 \\ C4 \end{bmatrix}$$

Let us denote w_j which is the number of detected adjacent chips "1" in the code matrix where j represent QoS index as: $j = H, M, L$. As shown in $ZCC - PTM_{4;5}$ code matrix, w_H of 5 (first row), w_M of 4 (fourth row), and w_L of 3 (second and third rows) are chosen for representing higher, medium, and lower QoS demand, respectively.

Figure 1 shows some periodic correlation functions (PCF) of the $ZCC - PTM_{4;5}$ code matrix: PACF of Code1 (C1) and the PCCF of (C1, C2), (C2, C3), and (C3, C4). The PACF and PCCF confirm that the set of codes is a ZCC set where the correlation functions satisfy:

$$\theta_{Ci,Cj}(\tau) = \begin{cases} w & i = j; \tau = 0 \\ 0 & i \neq j; \tau = 0 \\ < w & ; \tau \neq 0 \end{cases} \quad (11)$$

3. Salient features of the proposed code

The comparative performance of the proposed code with other existing constructions such as enhanced double weight (EDW), modified double weight (MDW), modified quadratic congruence (MCQ), and Pascal's triangle codes, at the same code length of 30, is tabulated in Table 1. It is noticed that EDW, Pascal's triangle, and proposed constructions generate an equal number of users with minimal cross-correlation which allows eliminating MAI.

The novel ZCC code based on the PTM matrix can be adapted to any weight and number of users by using a simpler, less complex, and more flexible construction

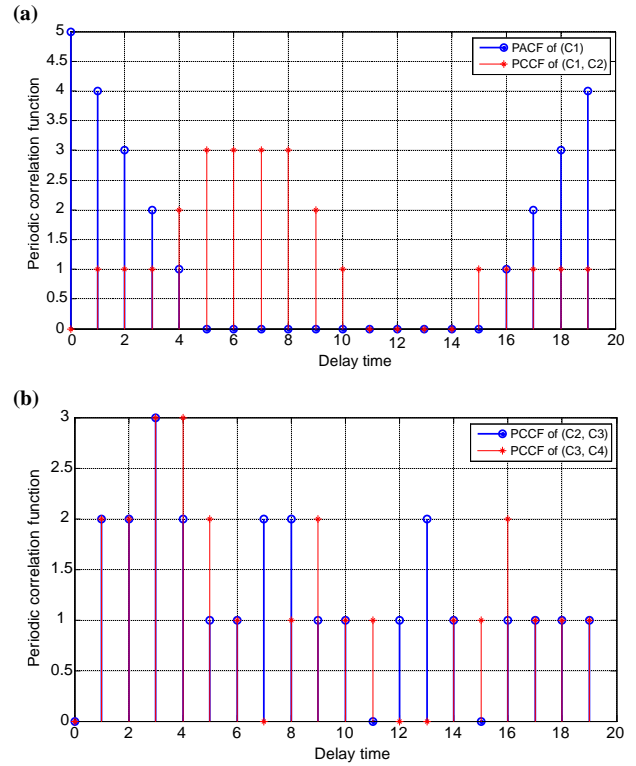


Fig. 1. PCF of codes C1 and C2 (a), PCCF of codes C2, C3, and C4 (b).

Table 1.
Comparison of the proposed ZCC-PTM code with some known OCDMA codes.

OCDMA Code	Weight	Length	Number of users	Cross correlation
EDW [25]	4	30	10	≤ 1
MDW [25]	16	30	9	1
MCQ [26]	6	30	25	1
Pascal triangle [22]	3	30	10	0
Proposed ZCC-PTM	3	30	10	0

procedure than others to provide bandwidth efficiency and full MAI elimination (cross-correlation = 0). On the other hand, because the chips "1" are adjacent, the ZCC-PTM code characteristics outperforms the code proposed in Ref. 22 such as:

- reduced number of filters used and system complexity, in the case of all-wavelengths direct detection, making the SAC-OCDMA systems more cost effective,
- compared to direct single wavelength detection, the signal-to-noise ratio (SNR) value is enhanced when increasing weight by using wide bandwidth filters as decoders,
- because of a variable number of detected adjacent chips "1" in the code matrix, the proposed construction is suitable for supporting multimedia applications with different service quality. In fact, to fulfil QoS differentiation property, codes with variable weight and longer code length are required [27–30]. This issue is resolved using the proposed code with constant weight and acceptable code length.

4. Performance analysis

4.1. Theoretical analysis

In order to evaluate the mathematical model of the bit error rate (BER) of OCDMA system based on the proposed ZCC-PTM code for the two direct detection (DD) schemes with detection of one wavelength (OW) and all wavelengths (AW) of the code, the Gaussian approximation is used. In the following analysis, only the effects of both shot and thermal noise are considered (due to the ZCC property). Consequently, the BER of the two DD schemes can be written as given below [31]:

in the case of OWDD,

$$BER = \frac{1}{2} \operatorname{erfc} \sqrt{\frac{1}{8} \cdot \frac{\left(\mathfrak{R} \cdot \frac{P_{sr}}{L}\right)^2}{2 \cdot e \cdot B \cdot \mathfrak{R} \cdot \frac{P_{sr}}{L} + \frac{4 \cdot K_b \cdot T \cdot B}{R_L}}}, \quad (12)$$

in the case of AWDD,

$$BER = \frac{1}{2} \operatorname{erfc} \sqrt{\frac{1}{8} \cdot \frac{\left(\mathfrak{R} \cdot P_{sr} \cdot \frac{w}{L}\right)^2}{2 \cdot e \cdot B \cdot \mathfrak{R} \cdot P_{sr} \cdot \frac{w}{L} + \frac{4 \cdot K_b \cdot T \cdot B}{R_L}}}, \quad (13)$$

where \mathfrak{R} denotes the responsivity of the photodetector, P_{sr} – the received effective power (−10 dBm), e – the electron charge (1.6×10^{-19} C), B – the electrical bandwidth, K_b – the Boltzmann’s constant (1.38×10^{-23} J/K), T – the receiver noise temperature (300 K), and R_L – the received load resistor (1030 Ω).

Figure 2 presents the performance comparison of the existing ZCC codes [22, 30–32] with OWDD and the proposed code in terms of BER against the number of simultaneous users at P_{sr} of −10 dBm. Due to the same ZCC property, the existing ZCC codes have the same BER performance which was enhanced by using the proposed code. Furthermore, by increasing the code weight, it can be noticed that the BER of the existing ZCC increases [see (12)], due to the increased code length. However, as the detected weight of the proposed code (w_L , w_M and w_H :

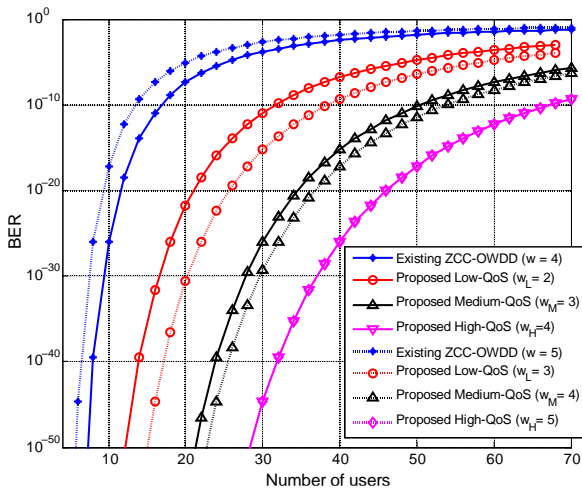


Fig. 2. BER comparison between the proposed code and other ZCC codes against number of users for OWDD.

number of detected wavelengths with one filter-based decoder) is increased, the received power increases without changing the code weight (the code length is kept fixed), which leads to a higher SNR and, thus, a better BER. Moreover, when the detected weight equals the weight of the code as in the case of ($w = 4$ and $w_H = 4$) or ($w = 5$ and $w_H = 5$), the same BER performances are obtained.

In the same manner as the OWDD, Figure 3 presents the performance comparison of the existing ZCC codes with AWDD and the proposed code in terms of BER against the number of active users at P_{sr} of −10 dBm. In this case, with the increasing code weight, the BER performances of the existing ZCC codes are similar to that of the proposed code for high-QoS [see (13) for $w = w_H$] with no BER changes for other detected weights (the same results as those in Fig. 2 with OWDD). However, the number of filters used in the decoder is reduced (only one optical filter) in the proposed scheme, thus, less complex architecture is obtained.

In order to further analyse the performance of the proposed ZCC-PTM code, Figure 4 shows the impact of the increasing data rate on the BER performance. For three different data rates (622 Mbps, 1.244 and 2.488 Gbps), it is observed that higher speeds lead to performance

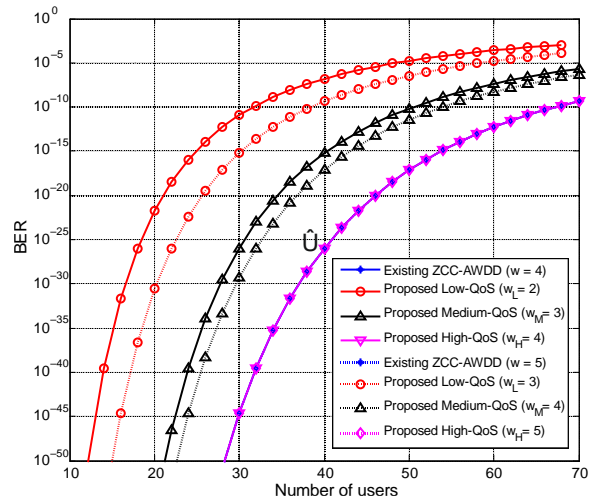


Fig. 3. BER comparison between the proposed code and other ZCC codes against number of users for AWDD.

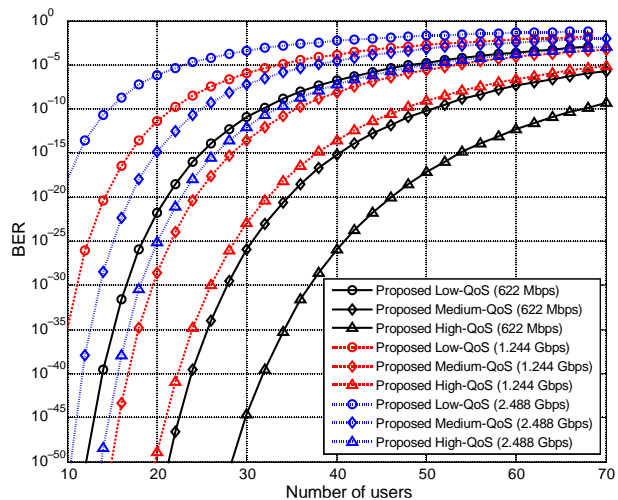


Fig. 4. BER performance of the proposed ZCC-PTM codes vs. number of users at different data rates.

degradation. Effectively, since the bit rate is proportional to the electrical noise bandwidth, an increased data bit rate causes more noise levels [shot and thermal noise, see (12) and (13)] and, thus, an increased BER.

Comparison of the proposed decoder and the AWDD scheme in terms of the number of filters used is given in Fig. 5. For the same user’s number and code weight, it is observed that the advantage of using the proposed ZCC-PTM code is obvious (fewer filters are used). This is because for AWDD the number of filters used equals the code weight while it is equal to 1 for any code weight in the proposed scheme.

The evaluation results shows that the proposed detection outperforms the AWDD and OWDD.

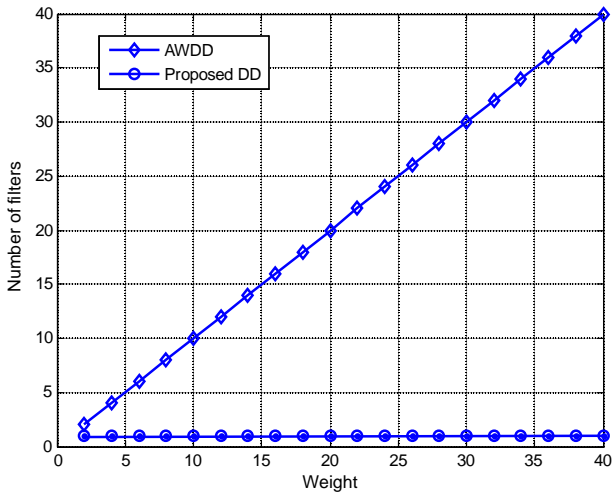


Fig. 5. Comparison of number of filters used at the decoder between AWDD and the proposed detection.

4.2. Simulation results

In this section, the effect of chips “1” position on the OCDMA system performance is evaluated by simulation using the OptiSystem software. Here, the performance of the system with the ZCC-PTM code is characterized in terms of the BER taking into consideration the simulation parameters shown in Table 2.

Table 2. Simulation parameters of the proposed ZCC-PTM OCDMA system.

Parameters	Value
Bit rate	622 Mbits/s 1.244 Gbits/s 2.488 Gbits/s
Spectral spacing	0.8 nm
Center frequency	192.69 THz
Number of users	5
Weight of the code	3
Fiber length	30 km
Fiber attenuation	0.2 dB/km
Fiber dispersion	18 ps/nm/km
Dark current	5 nA
Thermal noise	1.8×10^{-23}

In the simulation scheme and based on the optical carrier (OC) standard, established according to the synchronous digital optical network (Synchronous Digital Hierarchy/Synchronous Optical Network; SDH/SONET) model, the source is set to deliver the most popular OC services as: OC-12, OC-24 and OC-48 data rates (622 Mbits/s, 1.244 and 2.488 Gbits/s) [33, 34] for 5 active users.

The schematic block diagram of the proposed SAC-OCDMA system design is shown in Fig. 6.

The transmitter consists of an incoherent light source operating at a centre frequency of 192.69 THz (see Table 2) and five ZCC encoders to produce five user codes. Using ZCC – PTM_{5,3} code matrix defined beneath, each user requires three wavelengths with a 0.8 nm spacing to form his unique spectral signature (see Table 3).

$$ZCC - PTM_{5,3} = \begin{bmatrix} 0000 & 0000 & 111 & 0000 \\ 1000 & 000 & 1000 & 1000 \\ 0100 & 00 & 100000 & 0100 \\ 0010 & 01 & 00000000 & 010 \\ 0001 & 1000000000 & 0 & 1 \end{bmatrix}_{5 \times 15}$$

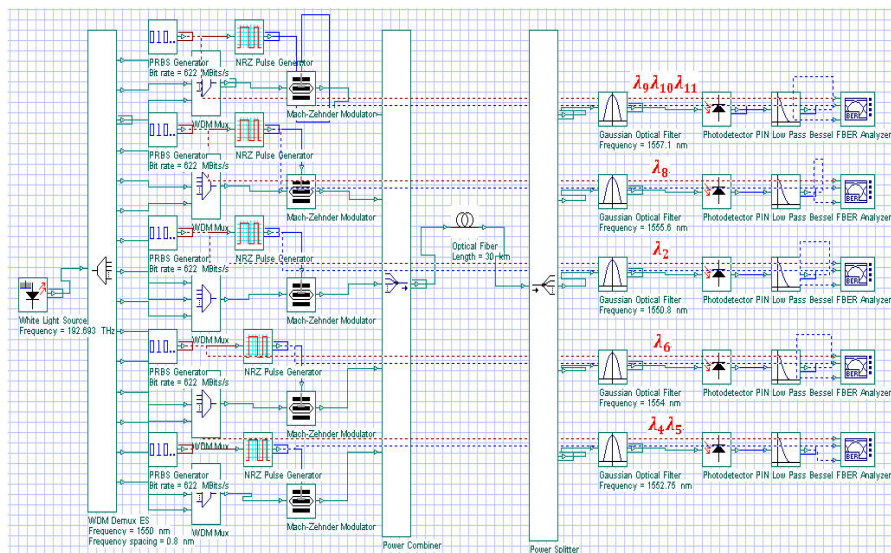


Fig. 6. ZCC-PTM OCDMA simulation setup for 5 users using direct detection.

Table 3.
Users' spectral signatures and their wavelength values.

	Code signature	Wavelength values
user 1	$\lambda_9\lambda_{10}\lambda_{11}$	(1556.4; 1557.2; 1558) nm
user 2	$\lambda_1\lambda_8\lambda_{12}$	(1550; 1555.6; 1558.8) nm
user 3	$\lambda_2\lambda_7\lambda_{13}$	(1550.8; 1554.8; 1559.6) nm
user 4	$\lambda_3\lambda_6\lambda_{14}$	(1551.6; 1554; 1560.4) nm
user 5	$\lambda_4\lambda_5\lambda_{15}$	(1552.4; 1553.2; 1561.2) nm

After modulating different data with different spreading sequences, they will be combined and sent to the receiver through 30 km of a single mode fibre (SMF). The fibre attenuation and dispersion were fixed as mentioned in Table 2.

The received signal is distributed to different decoders by a 1×5 power splitter. Further, the direct detection technique is applied to detect signals. However, due to the adjacent wavelengths (for the first and the last users in the studied example), multiple band pass filters (MBPFs) are used to transmit two or more channels (decode the received signal) with a single component. MBPF, commonly used in wavelength division multiplexing (WDM) channels [35, 36], offers many advantages such as cheaper alternative to one-chip optical filters that optimize the price-performance balance (simplifying design by minimizing component count and reducing component footprint).

For supporting multimedia services, optical Gaussian filters [30, 37] are used in the proposed variable-band direct detection scheme. The inherent properties of such filters (theoretical model as close as possible to the theoretical model of an ideal filter) make it a suitable candidate for recent SAC-OCDMA detection techniques providing better performance [30, 37]. In fact, while users 2, 3, and 4 detect one wavelength (λ_1, λ_2 , and λ_3 , respectively), user 1 detects the entire sent power (three adjacent wavelengths: λ_9, λ_{10} , and λ_{11} , simultaneously) and user 5 detects two adjacent wavelengths (λ_4 and λ_5).

At last, the obtained decoded signals are detected by a photodetector followed by low pass filters (LPFs).

The performance of the proposed OCDMA system in terms of BER are tabulated in Table 4. From the obtained results (see Table 4), it can be noticed that BER values of different users reach an acceptable BER threshold (less than the value of 10^{-9}) for a different data bit rate. In addition, for the same simulation parameters such as the number of users, code weight, bit rate, and link distance, fewer filters are used with the proposed ZCC-PTM code for a very low BER compared with the previously described codes.

As an example, the eye diagram of the user 1 is shown in Fig. 7 where three adjacent wavelengths are detected with one filter providing the best BER performance (see the case of 622 Mbits/s data rate in Table 4).

5. Conclusions

In this work, a novel ZCC code using the Pascal's triangle matrix suitable for multimedia applications has been proposed. The effectiveness of the proposed system is

Table 4.
Performance of the proposed ZCC-PTM OCDMA system.

Bit rate	User	Number of detected wavelengths	BER
622 Mbits/s	1	3	8.02002e-043
	2	1	1.48084e-026
	3	1	6.82083e-026
	4	1	4.81887e-026
	5	2	4.36389e-035
1.244 Gbits/s	1	3	1.24001e-024
	2	1	4.25200e-015
	3	1	8.74638e-014
	4	1	9.17856e-015
	5	2	2.65478e-020
2.488 Gbits/s	1	3	2.83638e-018
	2	1	2.81619e-010
	3	1	2.71201e-010
	4	1	3.11498e-010
	5	2	2.32993e-016

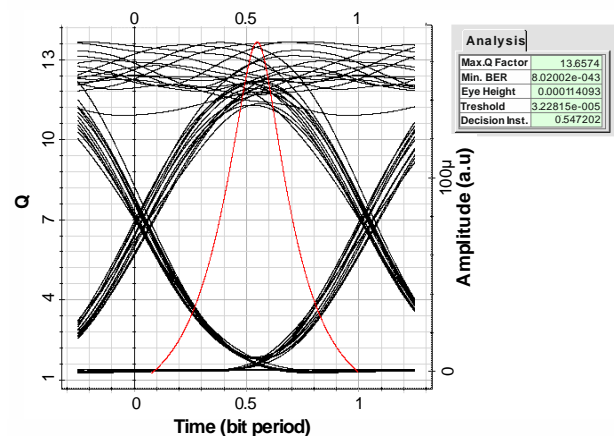


Fig. 7. Eye diagram of user 1 at data rate of 622 Mbits.

verified, analysed, and compared with the previous approach, using the OptiSystem software simulation in terms of the BER value. For the most used bit rates in practical scenarios, the suggested system obtains the best value of BER for higher and medium service demand, respectively due to the direct detection of more than one adjacent chip "1" in the code matrix. Numerical results show that the use of the proposed code outperforms the existing ZCC code [22] since it requires only multi band filters that improve bit error rate and optimize price-performance balance in optical networks vs. single band filters.

Authors' statement

Research concept and design, S. Driz, B. Fassi, and C. Kandouci; collecting and/or assembly of data, S. Driz, B. Fassi, and F. Ghali; data analysis and interpretation, S. Driz, B. Fassi, and C. Kandouci; writing the article, S. Driz, B. Fassi, and C. Kandouci; critical revision of the article, F. Ghali and S. Driz; final approval of article, S. Driz, B. Fassi, C. Kandouci, and F. Ghali.

Acknowledgements

This work was supported by Directorate General for Scientific Research and Technological development (DGRSDT). This research did not receive any specific grant from funding agencies in the public, commercial, or non-profit sectors.

References

- [1] Garba, A. A., Yim, R. M. H., Bajcsy, J. & Chen, L. R. Analysis of optical CDMA signal transmission: capacity limits and simulation results. *EURASIP J. Appl. Signal Process.* **10**, 1603–1616 (2005). <https://doi.org/10.1155/ASP.2005.1603>
- [2] Stok, A. & Sargent, E. H. The role of optical CDMA in access networks. *IEEE Commun. Mag.* **40**, 83–87 (2002). <https://doi.org/10.1109/MCOM.2002.1031833>
- [3] Chen, K. S., Chen, Y. C. & Liao, L. G. Advancing high-speed transmissions over OCDMA networks by employing an intelligently structured receiver for noise mitigation. *Appl. Sci.* **8**, 1–14 (2018). <https://doi.org/10.3390/app8122408>
- [4] Kaur, S. & Singh, S. Review on developments in all-optical spectral amplitude coding techniques. *Opt. Eng.* **57**, 116102 (2018). <https://doi.org/10.1117/1.oe.57.11.116102>
- [5] Gupta, S. & Goel, A. New bipolar spectral amplitude code for cardinality enhancement in OCDMA network. *J. Opt.* **49**, 1–8 (2020). <https://doi.org/10.1007/s12596-020-00589-4>
- [6] Driz, S. & Djebbari, A. Performance evaluation of sub-carrier multiplexed SAC-OCDMA system using optimal modulation index. *J. Opt. Commun.* **40**, 83–92 (2019). <https://doi.org/10.1515/joc-2017-0044>
- [7] Aldhaibani, A. O., Aljunid, S. A., Anuar, M. S. & Arief, A. R. Increasing performance of SAC-OCDMA by combine OFDM technique. *J. Theor. Appl. Inf. Technol.* **66**, 634–637 (2014).
- [8] Ouis, E., Driz, S. & Fassi, B. Enhancing confidentiality protection for ZCC-OCDMA network using line selection and wavelength conversion based on SOA. *J. Opt. Commun.* 000010151520200089 (2020). <https://doi.org/10.1515/joc-2020-0089>
- [9] Jyoti, V. & Kaler, R. S. Security enhancement of OCDMA system against eavesdropping using code-switching scheme. *Optik* **122**, 787–791 (2011). <https://doi.org/10.1016/j.ijleo.2010.05.027>
- [10] Moghaddasi, M., Seyedzadeh, S., Glesk, I., Lakshminarayana, G. & Anas, S. B. A. DW-ZCC code based on SAC-OCDMA deploying multi-wavelength laser source for wireless optical networks. *Opt. Quant. Electron.* **49**, 393 (2017). <https://doi.org/10.1007/s11082-017-1217-y>
- [11] Morsy, M. A. Analysis and design of weighted MPC in incoherent synchronous OCDMA network. *Opt. Quant. Electron.* **50**, 387 (2018). <https://doi.org/10.1007/s11082-018-1657-z>
- [12] Abd El-Mottaleb, S. A., Fayed, H. A., Aly, M. H., Rizk, M. R. & Ismail, N. E. An efficient SAC-OCDMA system using three different codes with two different detection techniques for maximum allowable users. *Opt. Quant. Electron.* **51**, 354 (2019). <https://doi.org/10.1007/s11082-019-2065-8>
- [13] Fassi, B. & Taleb-Ahmed, A. A. New construction of optical zero-correlation zone codes. *J. Opt. Commun.* **39**, 359–368 (2018). <https://doi.org/10.1515/joc-2017-0214>
- [14] Driz, S., Fassi, B., Mansour, M. A. & Taleb-Ahmed, A. FPGA implementation of a novel construction of optical zero-correlation zone codes for OCDMA systems. *J. Opt. Commun.* (2019). <https://doi.org/10.1515/joc-2019-0048>
- [15] Kandouci, C., Djebbari, A. & Taleb-Ahmed, A. A new family of 2D-wavelength-time codes for OCDMA system with direct detection. *Optik* **135**, 8–15 (2017). <https://doi.org/10.1016/j.ijleo.2017.01.065>
- [16] Ahmed, H. Y., Zeghid, M., Imtiaz, W. A., Sharma, T. & Chehri, A. An efficient 2D encoding/decoding technique for optical communication system based on permutation vectors theory. *Multimed. Syst.* **27**, 691–707 (2020). <https://doi.org/10.1007/s00530-020-00711-3>
- [17] Imtiaz, W. A., Ahmed, H. Y., Zeghid, M. & Sharief, Y. Two dimensional optimized enhanced multi diagonal code for OCDMA passive optical networks. *Opt. Quant. Electron.* **52**, 33 (2020). <https://doi.org/10.1007/s11082-019-2145-9>
- [18] Jellali, N., Najjar, M., Ferchichi & M., Janyani, V. Performance enhancement of the 3D OCDMA system by using dynamic cyclic shift and multi-diagonal codes. *Photonic Netw. Commun.* **37**, 63–74 (2019). <https://doi.org/10.1007/s11107-018-0793-5>
- [19] Anuar, M. S., Aljunid, S. A., Saad, N. M. & Hamzah, S. M. New design of spectral amplitude coding in OCDMA with zero cross-correlation. *Opt. Commun.* **282**, 2659–2664 (2009). <https://doi.org/10.1016/j.optcom.2009.03.079>
- [20] Nisar, K. S., Sarangal, H. & Thapar, S. S. Performance evaluation of newly constructed NZCC for SAC-OCDMA using direct detection technique. *Photonic Netw. Commun.* **37**, 75–82 (2019). <https://doi.org/10.1007/s11107-018-0794-4>
- [21] Kaur, R. & Kaler, R. S. Performance of zero cross correlation resultant weight spectral amplitude codes in lower Earth orbit-based optical wireless channel system. *Int. J. Commun.* **33**, e4456 (2020). <https://doi.org/10.1002/dac.4456>
- [22] Nisar, K. S., Djebbari, A. & Kandouci, C. Development and performance analysis zero cross correlation code using a type of Pascal's triangle matrix for spectral amplitude coding optical code division multiple access networks. *Optik* **159**, 14–20 (2018). <https://doi.org/10.1016/j.ijleo.2018.01.054>
- [23] Edwards, A. W. F. *Pascal's Arithmetical Triangle: The Story of a Mathematical Idea*. (Johns Hopkins University Press, 2002).
- [24] Németh, L. & Szalay, L. Power sums in hyperbolic Pascal triangles. *Analele Universitatii "Ovidius" Constanta-Seria Matematica* **26**, 189–203 (2018). <https://doi.org/10.2478/auom-2018-0012>
- [25] Kaur, S. & Singh, S. Review on developments in all-optical spectral amplitude coding techniques. *Opt. Eng.* **57**, 116102 (2018). <https://doi.org/10.1117/1.oe.57.11.116102>
- [26] Kumari, M., Sharma, R. & Sheetal, A. Performance analysis of high speed backward compatible TWDM-PON with hybrid WDM-OCDMA PON using different OCDMA codes. *Opt. Quant. Electron.* **52**, 1–59 (2020). <https://doi.org/10.1007/s11082-020-02597-x>
- [27] Zhao, H., Wu, D. & Fan, P. Constructions of optimal variable-weight optical orthogonal codes. *J. Comb.* **18**, 274–291 (2010). <https://doi.org/10.1002/jcd.20246>
- [28] Kakaee, M. H., Seyedzadeh, S., Fadhil, H. A., Anas, S. B. A. & Mokhtar, M. Development of multi-service (MS) for SAC-OCDMA systems. *Opt. Laser Technol.* **60**, 49–55 (2014). <https://doi.org/10.1016/j.optlastec.2014.01.002>
- [29] Kumawat, S. & Maddila, R. K. Development of ZCCC for multi-media service using SAC-OCDMA systems. *Opt. Fiber Technol.* **39**, 12–20 (2017). <https://doi.org/10.1016/j.yofte.2017.09.015>
- [30] Li, X. *et al.* Development and performance improvement of a novel zero cross-correlation code for SAC-OCDMA systems. *J. Opt. Commun.* 000010151520200086 (2020). <https://doi.org/10.1515/joc-2020-0086>
- [31] Garadi, A., Djebbari, A. & Taleb-Ahmed, A. Exact analysis of signal-to-noise ratio for SAC-OCDMA system with direct detection. *Optik* **145**, 89–94 (2017). <http://doi.org/doi:10.1016/j.ijleo.2017.07.038>
- [32] Imtiaz, W. A., Ilyas, M. & Khan, Y. Performance optimization of spectral amplitude coding OCDMA system using new enhanced multi diagonal code. *Infrared Phys. Technol.* **79**, 36–44 (2016). <https://doi.org/10.1016/j.infrared.2016.09.006>
- [33] Rec, I. T. U. (1988). G. 707: Synchronous Digital Hierarchy - Bit Rates. International Telecommunication Union, ITU-T. (1988).
- [34] Kartalopoulos, S. V. *Communication Networks*. in Next Generation Intelligent Optical Networks, from Access to Backbone. (Springer, Boston, MA, 2008). <https://doi.org/10.1007/978-0-387-71756-2>
- [35] Calligaris Jr, A. O. & Silva, M.T.C. Multichannel Bandpass Optical Filter Integrated in Tandem For High-Speed Wavelength Division Multiplexed Systems. *Revista Científica Periódica-Telecomunicações*. **2**, 28-29(1999). <https://www.inatel.br/revista/downloads/marco-setembro-1999-s883750-1>
- [36] Naghar, A., Aghzout, O., Alejos, A. V., Sanchez, M. G. & Essaaidi, M. Design of compact wideband multi-band and ultra-wideband band pass filters based on coupled half wave resonators with reduced coupling gap. *IET Microw. Antennas Propag.* **9**, 1786–1792 (2015). <https://doi.org/10.1049/iet-map.2015.0188>
- [37] Abdulqader, S. G., Fadhil, H. A., Aljunid, S. A. & Safar, A. M. Performance Analysis of an OCDMA System Based on SPD Detection Utilizing Different Type of Optical Filters for Access Networks. in *Advanced Computer and Communication Engineering Technology*. (Cham Springer International Publishing, 2015). https://doi.org/10.1007/978-3-319-07674-4_31